DATA APPENDIX

Contents:

A

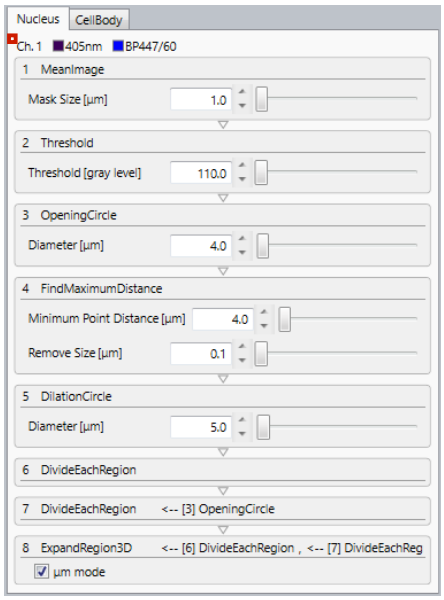

1. Detection of distinct nuclei.

(1) Image smoothening

(2) Image binarization by applying a user-defined threshold*

(3) Edges of detected objects are smoothened

(4) Only objects with a user-defined minimal distance to adjacent objects are considered for further analysis to avoid double counting. The centers of these objects are labeled.

(5) The label of detected objects is enlarged for better visualization

(6-7) All filtered objects are included

(8) Labeled nuclei are 3 dimensionally expanded to their edges

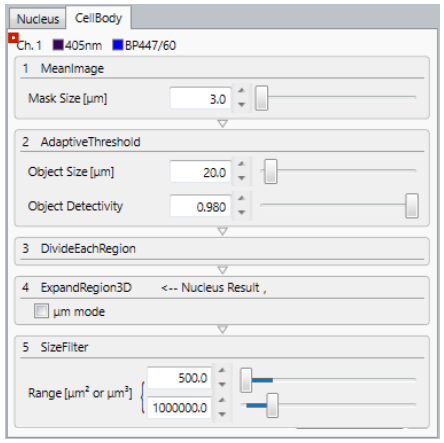

2. Segmentation of adjacent cells.

(1) Image smoothening

(2) Image binarization and application of a size threshold for objects

(3) Designation of distinct objects

(4) Objects detected above (analysis 1 and 2) are expanded in 3D to segment adjacent cells

(5) Only objects greater than 500 µm^3 are considered

B

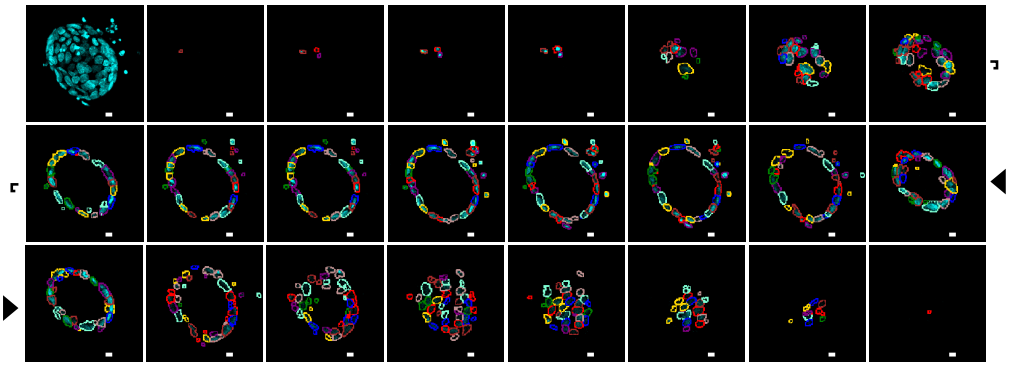

Appendix Figure S1. Image-based analysis to determine absolute organoid cell number

A) Analysis algorithm using the CQ1 software. The application 'Spheroid Structure' was first used to determine the organoid cell number based on DAPI signals (top) followed by segmentation of individual nuclei (bottom). *: for optimal recognition the threshold was adjusted for each well separately.
B) Sample data for the analysis of one representative organoid. Maximum image projection (top left) and individual z stacks are shown. Automatically detected nuclei in each image are outlined in color. For cells spanning various z-stacks the color remains constant. Scale bars: 50 µm.

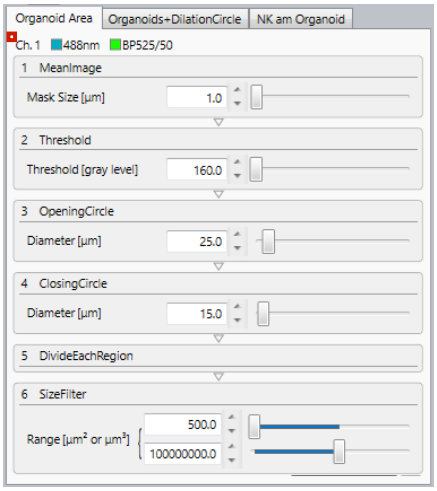

1. Detection of organoids.

(1) Image smoothening

(2) Image binarization by applying a user-defined threshold*

(3-4) Noise reduction at the edge of detected objects*

(5) All detected objects are designated as distinct objects

(6) Only objects greater than 500 µm^2 are considered for further analysis

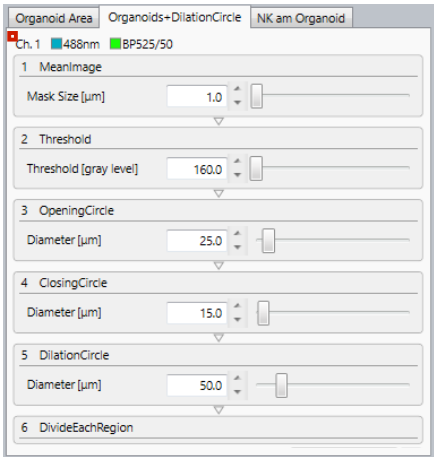

2. Addition of a dilation circle to detected organoids.

(1-4) As described above

(5) Detected objects are expanded by addition of a dilation circle.

(6) All expanded objects are designated as distinct objects and assigned an individual object ID

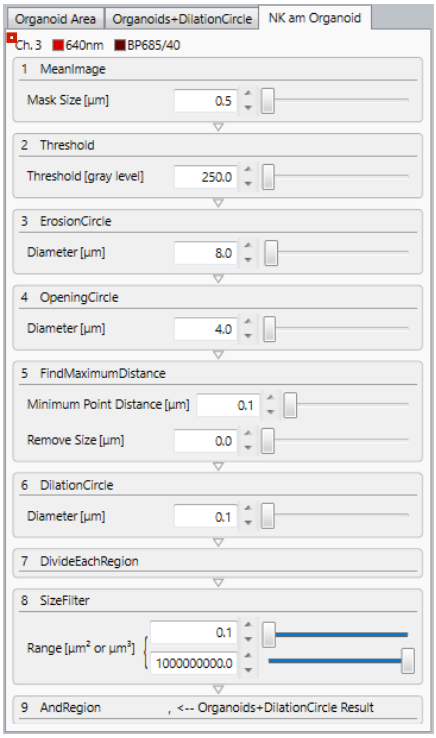

3. Counting of NK-92 cells within the dilated organoid area.

(1) Image smoothening

(2) Image binarization by applying a user-defined threshold*

(3-4) The area of detected objects is reduced to separate individual objects

(5) Objects were reduced to points with maximum distance from their edges. Only objects with a user defined minimum distance to adjacent objects are considered for further analysis to avoid double counting

(6) Objects detected by then are assigned a user-definded artifical diameter. Objects of this size are further recognized and counted

(7) All detected objects are designated as distinct objects

(8) Size filtering is adjusted to detect objects of the size set in (6)

(9) Limiting the detection and counting of objects to the expanded organoid area (Only objects detected in (8) which are additionally located in a dilated organoid area (Analysis level 2) are counted)

Appendix Figure S2. Image-based analysis of organoid area and NK-cell recruitment

Analysis algorithm using the CQ1 software. First the organoid area was determined from GFP signals (top panel). Then a recruitment area was defined by expanding the organoid areas with a constant diameter of 50 µm (middle panel). In this expanded area all CD45-APC positive NK cells were counted using a third level of analysis (bottom panel). *: for these steps adjustments were set for each well separately.

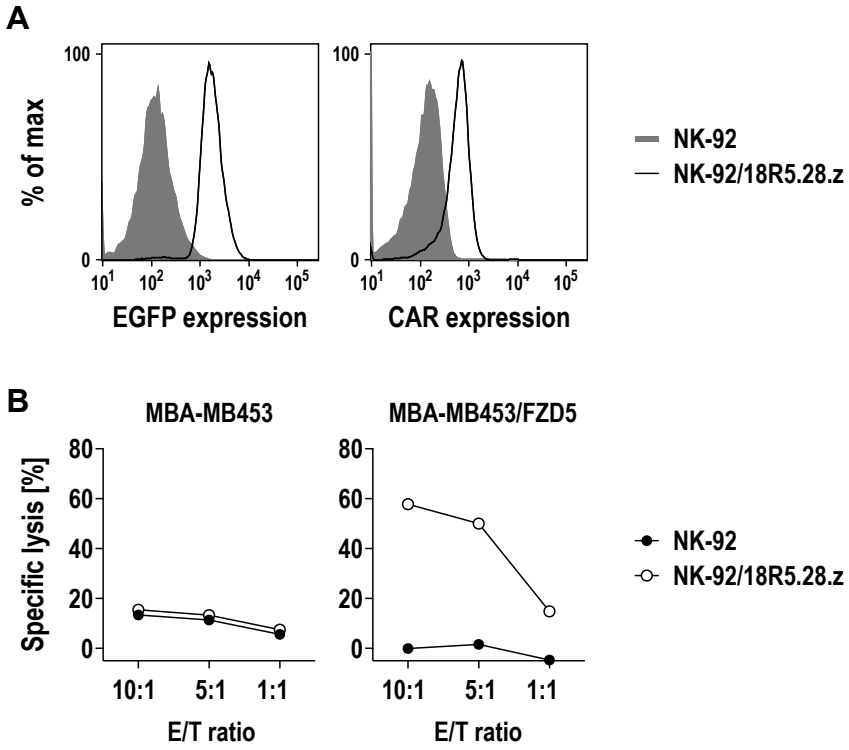

Appendix Figure S3. Generation and characterization of pan FZD-CAR NK-92 cells

A) Expression of the FZD-CAR and the co-expressed GFP in transduced NK-92 cells was studied by flow cytometry. CAR expression was detected with Myc-tag-specific antibody. Parental NK-92 cells were included as control.
B) Cytotoxic activity of FZD-CAR NK-92 cells against MDA-MB453 cells stably expressing FZD5. Parental MDA-MB453 and NK-92 cells were used as controls.

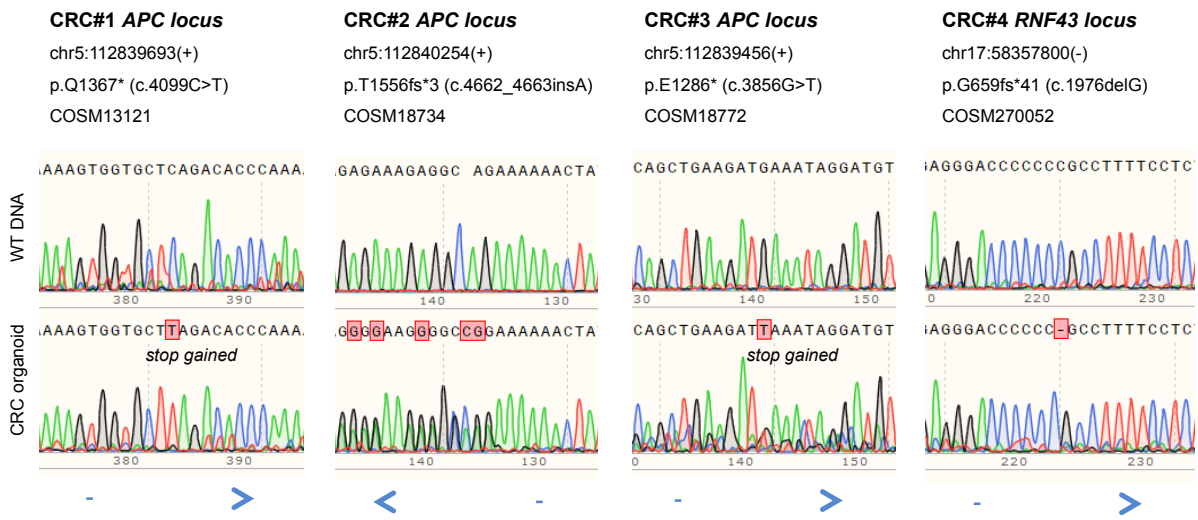

Appendix Figure S4. *RNF43* and *APC* genotyping of human CRC organoids

Sanger sequencing spectrograms using genomic DNA from WT (top) and CRC organoids (bottom) identifies damaging coding mutations in the *APC* locus (CRC#1-3) or in *RNF43* (CRC#4). For all lines the *APC* mutation cluster region (1132 bp) and for *RNF43* a recurrently mutated region (1244bp; Giannakis et al., 2014) was analyzed and no additional mutations were identified. Genomic coordinates (hg38) and protein consequences and COSMIC mutation IDs are indicated. The synthesis direction of sequencing is indicated by the blue arrow.